32ND INTERNATIONAL COSMIC RAY CONFERENCE, BEIJING 2011

Charged-Particle Transport in anisotropic magnetic Turbulence

P. SUN AND J. R. JOKIPII
Department of Planetary Sciences, University of Arizona, Tucson, Arizona, USA
pengsun@lpl.arizona.edu

Abstract: Turbulence with an associated turbulent magnetic field is common in astrophysical environments. The determination of the transport of charged particles both parallel and perpendicular to the mean magnetic field is of considerable interest. Quasi-linear analysis or direct numerical simulation can be used to find the effects of the turbulent magnetic field on the transport of charged particles. A number of different magnetic turbulence models have been proposed in the last several decades. We present the results of studying particle transport in synthesized, anisotropic (Goldreich & Sridhar, 1995) turbulence and compare the results with those obtained using the standard isotropic turbulence model.

Keywords: Transport, Magnetic turbulence, anisotropy

1 Introduction

The scattering and diffusion of energetic charged particles is not only important for understanding phenomena such as diffusive shock acceleration but it also is a natural probe of the statistical characteristics of magnetohydrodynamics (MHD) turbulence. Although Parker's transportation equation [1] allows us to describe the propagation of charged particles, the transport coefficients needed in the equation must be determined. Quasi-Linear Theory (QLT[2]) shows that coefficients can be related to the correlation function of isotropic homogeneous magnetic turbulence, which shows the important role of Field Line Random Walk (FLRW[3]). However, the statistics in different turbulence models will generally have different influences on the particle's scattering and diffusion. Among those models developed on MHD Turbulence such as isotropic Slab [4], Slab plus 2D [5, 6] , etc., a Kolmogorov type, incompressible one, first proposed by [7] is chosen in this test particle simulation to calculate the transport coefficients in the tensor.

Anisotropy in MHD turbulence was proposed nearly 30 years ago [8]. And observations have also shown the anisotropy in the solar wind turbulence[9, 10]. In the Goldreich-Sridhar model, for incompressible turbulence, in the inertial range the turbulence cascade is also anisotropic. The mixing of perpendicular motion and parallel waves are connected by $k_{\|}V_A \sim k_{\perp}v_k$, where $k_{\|}$ is the parallel motion component wave number, V_A the Alfven speed, $k_{\perp}$ the perpendicular motion component wave vector, v_k the speed of the motion. This "critical balance" between $k_{\|}$ and $k_{\perp}$ in the local reference frame is assumed based on that: 1) the parallel wave modes are traveling at Alfven speed along the field line while the normal components at speed v_k, 2) the parallel cascading time scale is $(k_{\|}V_A)^{-1}$ while the perpendicular cascading time scale is $(k_{\perp}v_k)$ and, 3) these two time scales are equal to each other, which is the critical balance condition. At this mixing rate the cascading energy would be equally partitioned in both direction. This anisotropy changes the magnetic field and hence could modify the scattering and diffusion of energetic particles from the isotropic case, which is of great interest.

Recently, test particle simulations were performed by Berensnyak et al 2011[11] using results from MHD turbulence simulation. Our approach is different from theirs in that it not only preserves the statistics of the magnetic turbulence such as moments (mean, variance) and correlation functions (power spectra), but also, because of the synthesizing method, explores the full range of scales in the inertial region. Alternatively, this could be achieved by interpolation in Direct Numerical Simulations of turbulence but only with limited resolution.

In this paper we compare the influence of the anisotropic turbulence to the transport of charged energetic particles with previous turbulence models in the context of protons with energy from $1MeV \sim 1GeV$ traveling in the solar wind. Section 2 describes the method used to generate the turbulent magnetic field. Section 3 lists the parameters used in simulation. Section 4 shows the results and section 5 is discussion.

2 Magnetic turbulence

The static magnetic field which we used is synthesized using a method similar to that used in Giacalone et al [12] (hereafter referred as label12) for isotropic and com-

posite turbulence. Here we use the power spectrum function at wave number $k_\perp$ and $k_\parallel$ with $P(k_\perp, k_\parallel) \sim (k_\perp)^{-10/3} f(k_\parallel/k_\perp^{2/3})$, where $k_\parallel$ is the parallel motion component wave number and, $k_\perp$ the perpendicular motion component wave vector[7]. To take into account of the large scale magnetic field meandering, we adapt an asymptotic function of $k_\perp^{-10/3}$. For the function $f(L^{1/3}k_\parallel/(k_\perp)^{2/3})$, which dictates the critical balance between $k_\parallel$ and $k_\perp$ in the local reference frame, we take the exponential form[13]. The spectrum function used in the simulation is listed as follow

$$P_1(k_\perp, k_\parallel) = \frac{\sigma_B^2 L^3 \exp\{-L^{1/3}|k_\parallel|/(k_\perp)^{2/3}\}}{6\pi(k_\perp L)^{5/3}(1+k_\perp L)^{5/3}} \qquad (1)$$

Where σ_B^2 is the variance of the magnetic field strength and L is the turbulence injection length. If the power (P_1) is small, the spectrum turns to be isotropic. As the power (P_1) increases, it turns to elongate along $k_\perp$, which is the direction normal to the mean field. This anisotropy corresponds with what would be expected in Goldreich-Sridhar type spectrum. If power spectrum is integrated over $k_\parallel$ to be a function only of $k_\perp$, the 1-D power spectrum index is $-5/3$, as expected as the Kolmogorov power spectrum. The power function P_2 is similar.

3 Tracking test particles

3.1 Trajectory integration

Since the energetic particles have a much lower density than the thermal particles and a test particle simulation is adequate. The motion of the charged particles is governed by the Lorentz force:

$$\frac{d\mathbf{v}}{dt} = \frac{q}{mc}\mathbf{v} \times \mathbf{B} \qquad (2)$$

where q is the charge, m the mass, **v** the velocity, and c the speed of light.

We solve this equation using a fourth order, adaptive-step Ronge-Kutta method ([14]). Each step is calculated by 5 sub-points within the step. And each step size is adjusted to preserve the given step error tolerance. So if the equation is smooth, the time step can be relatively large. If the parameters vary rapidly, the time step shrinks accordingly. Although it is not a conservative method (for accumulative truncation error), as in this simulation, the time step is around $10^3\Omega_i^{-1}$(ion gyrofrequency) , which means the truncation error is tolerable compared with the real solution.

For each case listed in table 1, we used 2400 particles and 48 realizations of magnetic field with different sets of random wave modes as mentioned in the last section. And for each realization there are 50 particles set with the same initial speed and position but in different directions isotropically distributed.

Simulation Parameters

#	E	r_g	σ^2	L_c	λ_{min}	λ_{max}
-	MeV	10^{-3}AU	AU	r_g	r_g	r_g
1	1.0	0.193	1.0	51.9	0.519	5190
2	3.16	0.343	1.0	29.2	0.2917	2917
3	10.0	0.611	1.0	16.4	0.1637	1637
4	31.6	1.09	1.0	9.15	0.0915	915.4
5	100	1.98	1.0	5.06	0.0506	505.8
6	316	3.70	1.0	2.70	0.0270	270.0
7	1000	7.59	1.0	1.33	0.0133	132.6
8	31.6	1.09	0.5	9.15	0.0915	915.4
9	31.6	1.09	0.3	9.15	0.0915	915.4
10	31.6	1.09	0.1	9.15	0.0915	915.4
11	31.6	1.09	0.05	9.15	0.0915	915.4
12	31.6	1.09	0.01	9.15	0.0915	915.4

Table 1: All the cases are calculated in Goldreich Sridhar type turbulence spectrum.

The transport coefficients are calculated in the same way as in label12 by fitting the solution to a finite absorbing boundary diffusion problem.

3.2 Parameters

Listed in Table 1 are simulation cases and related parameters. They are the same as in [12]. The variance of the turbulence magnetic field is 1.0 in case 1 to 7 and varies in case 4 and 8 to 12.

4 Results

Table 2 shows the result of the simulations.

Simulation Results

Case	$\kappa_\perp$	$\kappa_\parallel$	$\kappa_\perp/\kappa_\parallel$
-	$10^{18}\frac{cm^2}{s}$	$10^{20}\frac{cm^2}{s}$	1
1	3.224	1.043	0.031
2	6.434	2.200	0.029
3	11.39	4.791	0.024
4	27.06	12.49	0.022
5	53.47	27.22	0.020
6	118.3	67.20	0.018
7	234.3	163.4	0.014
8	16.76	25.71	0.0065
9	10.41	72.86	0.0014
10	8.691	121.8	0.0007
11	5.933	217.0	0.0003
12	1.457	345.6	4.2×10^{-5}

Table 2: The results are from the correspondent cases using GS[7] type turbulence spectrum as equation (1).

Figure 1 shows how the $\kappa_\perp$, $\kappa_\parallel$ (left panel) and $\kappa_\perp/\kappa_\parallel$ vary with particle's energy, as in case 1 to 6 in table 1. Both

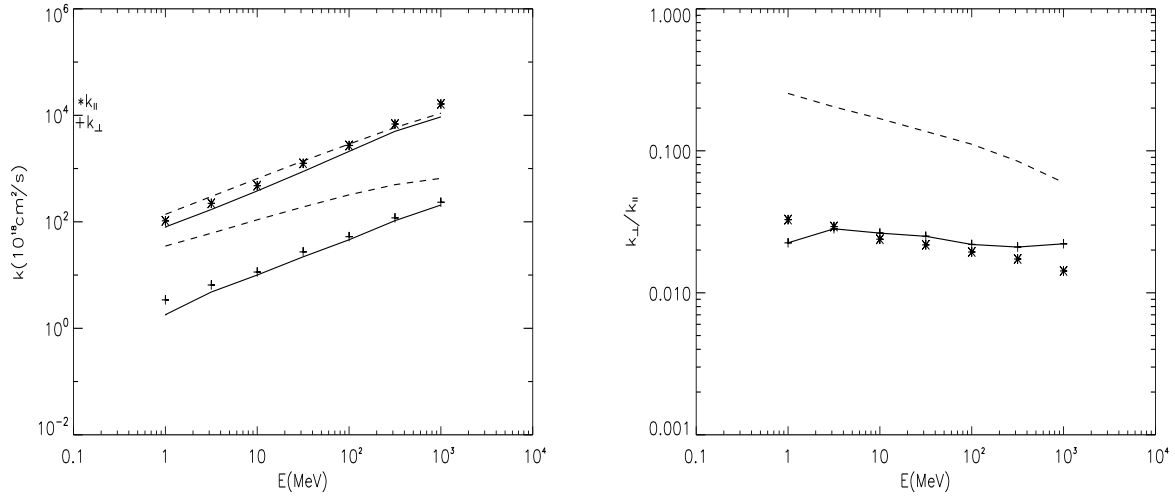

Figure 1: The left panel shows perpendicular and parallel transport coefficients in both GS type and isotropic turbulence spectrum, as a function of the particle's energy. The stars and crosses, $\kappa_\perp$ and $\kappa_\parallel$ respectively, are values in Table 2. The solid lines are simulation results from cases with the isotropic turbulence power spectrum as in Giacalone et al [12]. The upper one is the parallel diffusion coefficient while the lower one the perpendicular coefficient. The upper and lower dashed lines are the coefficients calculated by equations 3 and 5 respectively. The right panel shows their ratio as the function of proton energy. Stars are $\kappa_\perp/\kappa_\parallel$'s from Table 2. And the crosses connected by the solid line represents simulations results with isotropic turbulence model, and the dashed line is from equations (3) and (5) using GS type power spectrum. All the results as according to the cases 1 to 7 in Table 1.

coefficients increase with particle's energy, and the magnitude of these two coefficients are close to those calculated in label12 from isotropic (and composite) turbulence spectrum. According to Quasi-Linear Theory, the perpendicular coefficient is [2]

$$\begin{aligned}\kappa_\perp &= \frac{1}{2}\int_0^1 d\mu\{\frac{\mu v}{B_0^2}P_\perp(k_\perp=0) \\ &\quad +\frac{(1-\mu^2)v}{2|\mu|B_0^2}P_\parallel(k_\parallel=\frac{\Omega_0}{\mu v})\} \\ &\cong \frac{vL_c}{6}\frac{\sigma_B^2}{B_0^2} \end{aligned} \quad (3)$$

A quick estimate would tell us the dominate effect in both isotropic and Goldreich-Sridhar type turbulence is in the low wave number components. In the simulation it is expected to be lower than the estimate by the Quasi-Linear Theory because we start from $k = 0.1(Lc^{-1})$. In the parallel diffusion case, the scattering rate and diffusion coefficient could be calculated by [2, 15, 16]

$$\nu = \frac{2D_{\mu\mu}}{1-\mu^2} = \frac{\pi}{3}\Omega_0\frac{\sigma_B^2}{B_0^2}\frac{\frac{\Omega_0 L_c}{(v|\mu|)}}{(1+\frac{\Omega_0 L_c}{v|\mu|})^{5/3}} \quad (4)$$

$$\kappa_\parallel = \frac{3v^3}{\pi\Omega_0^2 L_c}\frac{B_0^2}{\sigma_B^2}\int_0^1 \mu(1-\mu^2)(1+\frac{\Omega_0 L_c}{v\mu})^{5/3}d\mu \quad (5)$$

The values from simulation are close to the estimate from equation 5. The ratio $\kappa_\perp/\kappa_\parallel$, unlike in the isotropic turbulence case, decreases slightly with particle's energy, as shown in Figure 1. If we compare equation 3 to equation 5, we could see the ratio of transport is related to v^2. However, it does not change much. As in the particle's energy range ($1MeV \sim 1GeV$) we tested, it is about $0.01 \sim 0.03$ for a strong turbulence ($\sigma_B^2 \sim 1$), or $\kappa_\perp << \kappa_\parallel$. In Figure 2, this ratio is even smaller for milder turbulence variances.

Furthermore, in the Goldreich-Sridhar type turbulence, the perpendicular diffusion coefficients are larger than that in isotropic type. Since it is mainly controlled by the large scale field component, the perpendicular transport coefficients calculated in the simulation in both Goldreich-Sridhar type and isotropic case are very close to each other. This just confirms the Field Line Random Walk theory proposed by [2] and [3] on particle's transverse motion.

Notice also that $\nu \sim (v\mu)^{2/3}\sigma_B^2$, then by Quasi-Linear Theory, it is zero at pitch angle $\theta = 90^0$ and would maximize at $\theta \sim 0^0$. Also it increases with particle's energy and the variance of magnetic turbulence . This could be related to the magnetic mirror effect induced by the fast mode wave in the turbulence, which will increase the scattering rate. While scattering rate is very important in diffusive shock acceleration, one might estimate that in turbulence model with strong fast mode related cascading, the acceleration will be enhanced.

Figure 2 shows how the $\kappa_\perp$, $\kappa_\parallel$ (left panel) and $\kappa_\perp/\kappa_\parallel$ vary with the variance of the magnetic field, as the particle's energy is 31.6 MeV. In the left panel of figure 2 it shows the perpendicular transport coefficient increases as the variance of the magnetic field increases, since in this case both the scattering and field line random walk are stronger. The

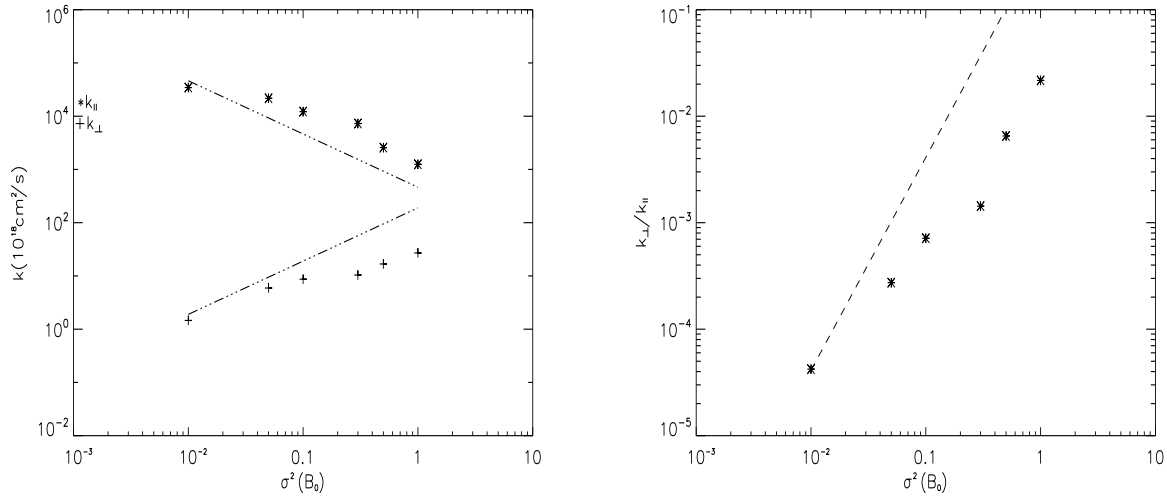

Figure 2: In the left panel, stars and crosses show perpendicular and parallel transport coefficients from Table 2, as a function of variance of the field strength. Similar to Fig.1, The upper and lower dashed-dotted lines are from test particle simulations with the isotropic power spectrum[12] for perpendicular and parallel diffusion coefficients respectively. In the right panel, stars show the ratio of $\kappa_\perp$ to $\kappa_\parallel$ from Table 2 varies with the variance of the field strength while the dashed line represent the calculation from equations (3) and (5). The results are according to the case 4 and 8-12 in Table 1.

parallel transport coefficient is smaller, since the mean free path in this case along the field line would be smaller. Combine these two changes, the ratio of transport coefficient, $\kappa_\perp/\kappa_\parallel$, is then increasing as the variance is enlarged.

5 Conclusion

Using the global Goldreich&Sridhar power spectrum we constructed an globally anisotropic turbulent magnetic field and performed test particle simulation to analyze particle's diffusion and the conclusions could be summarized as follows:

1. There is no big difference on particle's diffusion between isotropic and globally anisotropic turbulence magnetic fields; Field Line Random Walk is sill the main factor of particle's diffusion;

2. The ratio $\kappa_\perp/\kappa_\parallel$ is about $0.01 \sim 0.03$ for a strong turbulence ($\sigma_B^2 \sim 1$); and

3. $\kappa_\perp \sim \sqrt{E}\sigma_B^2$, $\kappa_\parallel \sim \sqrt{E^3}(\sigma_B^2)^{-1}$.

However, the synthesized magnetic turbulence is globally anisotropic. One of the main feature of GS95 model is that the magnetic turbulence may be local. In other words, the nearly spherical turbulence eddy in the large scale (say, the turbulence injection scale), would stretch along the local mean magnetic field line to the shape of a highly elongated spheroid in smaller and smaller scales in the turbulence inertial range.

Therefore, one has to determine the local average field direction when adding the parallel and perpendicular wave components in different scales ($|k_\parallel| \sim k_\perp^{2/3}$). One of the difficulties arises from the fact that when one is doing the synthesize, the average field would be changed accordingly. In the same time, the local critical balance condition ($|k_\parallel| \sim k_\perp^{2/3}$) and zero-divergence condition ($\nabla \cdot \mathbf{B} = 0$) have to be maintained. How to incorporate the localized feature in the synthesized magnetic field and how would the anisotropic turbulence affect the transport of charged particles will be the next step of this work.

References

[1] Parker, E. N., 1965, PSS, 13: 9
[2] Jokipii, J. R., ApJ, 1966, 146: 480
[3] Jokipii, J. R., & Parker, E. N., 1969, ApJ, 155: 777
[4] Tu, C. Y. et al, 1993, J. Geophys. Res., 98: 1257
[5] Gray, C. et al, 1996, Geophys. Res. Lett., 23: 965
[6] Bieber, J. W. et al, 1996, J. Geophys. Res., 101: 2511
[7] Goldreich, P. & Sridhar, H., 1995, ApJ, 438: 763
[8] Shebalin, J. V. et al, 1983, J. Plasma Phys., 29: 525
[9] Matthaeus, W. H. et al, 1990, JGR, 95: 20673
[10] Horbury, T. S. et al, 2008, PRL, 101: 175005
[11] Beresnyak, A. et al, ApJ, 2011, 728: 60
[12] Giacalone, J., & Jokipii, J. R., 1999, ApJ, 520: 204
[13] Cho, J. et al, 2002, ApJ, 564: 291
[14] Press, W. H. et al, Numerical Recipes, 1986, Cambridge:Cambridge Univ. Press
[15] Earl, J. A. 1974, ApJ, 193: 231
[16] Luhmann, J. G. 1976, J. Geophys. Res., 81: 2089